REDUCTION OF CAVITY PULLING IN A PASSIVE HYDROGEN MASER

W.M. Golding*, V.J. Folen, A.F. Frank, J.D. White, R.L. Beard
Naval Research Laboratory
Washington D.C. 20375

ABSTRACT

A new method for detection of the hydrogen resonance in a passive maser, has been tested and experimentally verified. This technique, which reduces the effect of cavity pulling on system performance, makes use of several amplitude and phase measurements of the combined transfer function associated with the cavity and hydrogen line. The atomic resonant frequency, determined in this way, has been shown to be essentially free from cavity pulling. For example, we have measured pulling factors 40 times lower than those measured using pure amplitude or phase techniques for the detection of the hydrogen resonance. The smaller cavity pulling factor is important in systems where cavity tuning errors are thought to yield an intrinsic limit on overall clock performance. The technique can be useful as a diagnostic tool, or as the hydrogen resonance detection method in an operational passive maser.

INTRODUCTION

This paper will show that sampling at discrete frequencies both the phase and amplitude of the forward transfer function of a passive hydrogen maser can yield a discriminator characteristic which is essentially free from cavity pulling. This approach reduces the severe requirements placed on the cavity servo in a passive system. The nominal pulling factor, when detecting by standard techniques, is proportional to the ratio of the cavity Q to the hydrogen line Q. In our system, which is a miniature passive hydrogen maser, this pulling produces 2×10^{-14} fractional frequency error per hertz of cavity tuning error. Therefore, to meet long term stability goals of 1×10^{-15}, we require that the cavity, the nominal resonant frequency of which is $1420.405 MHz$, be controlled to $\approx 0.050\ Hz$. Control of the cavity resonator to this degree requires extremely stable and accurate measurement of the resonance, along with the ability to tune the resonance in a way which does not degrade the measurement accuracy. This can be difficult to achieve and maintain. Utilizing sampling of the phase and amplitude of the forward transfer function, we have designed a system to lock to the hyperfine frequency rather than some specific characteristic of the overall transfer function, such as the maximum of the amplitude response. This design has yielded a reduction of cavity pulling by a factor of 40 in our present system. With further development, we hope to be able to reduce the pulling factor to the extent that the cavity servo will no longer be critical, thereby simplifying the implementation of a passive system.

THE MASER TRANSFER FUNCTION

In the paper by Viennet, Audoin and Desaintfuscien [1] and also in the paper by Lesage and Audoin [2], a useful model for the steady state response of a hydrogen maser is given. The model assumes that the atomic medium obeys the Bloch equations. The resonant microwave cavity of the model is driven by both the induced magnetization of the atomic hydrogen, and by an interrogating field.

The scattering parameters for the maser are derived largely from the the references [1] and [2]. The negative impedance concepts are well explained in [3]. The normalized forward transfer function for a two port maser, driven by a matched generator, and driving a matched load is derived in [1] and [2]. We have used this transfer function to fix the parameters of the equivalent circuit shown in figure 1. The relevant parameters of the equivalent circuit are the cavity impedance Z_c and the negative atomic impedance Z_a. For the angular frequency of the probing signal ω, near to both the cavity (ω_c) and hydrogen (ω_0) resonances, one obtains

---

* Sachs/Freeman Associates, Landover, MD

$$Z_c(\omega) \cong R_c(1 + jT_{cu}(\omega - \omega_c)) \tag{1}$$

$$Z_a(\omega) \cong \frac{-R_a}{1 + jT_2(\omega - \omega_0)}. \tag{2}$$

It is convenient to normalize both Z_c and Z_a to R_c. We define $\hat{Z}_c \equiv Z_c/R_c$ and $\hat{Z}_a \equiv Z_a/R_c$. The coupling parameters β_1 and β_2 are,

$$\beta_1 = \frac{n_1^2 Z_0}{R_c} \quad and \quad \beta_2 = \frac{n_2^2 Z_0}{R_c}, \tag{3}$$

where Z_0 is the characteristic impedance of the external transmission lines, and R_c is the resistive part of the cavity impedance. The ideal transformer ratios are n_1 and n_2. We define the normalized generator impedance as $\hat{Z}_g \equiv Z_g/Z_0$ and the normalized load impedance as $\hat{Z}_l \equiv Z_l/Z_0$.

From this equivalent circuit, the complete set of scattering parameters for the two port maser can be calculated. The scattering parameters are found to be,

$$S_{11} = \frac{\nu_{11} + jT_c(\omega - \omega_c) - \frac{\alpha}{1+S}/(1 + jT_2(\omega - \omega_0))}{1 + jT_c(\omega - \omega_c) - \frac{\alpha}{1+S}/(1 + jT_2(\omega - \omega_0))} \tag{4}$$

$$S_{21} = \frac{\nu_{21}}{1 + jT_c(\omega - \omega_c) - \frac{\alpha}{1+S}/(1 + jT_2(\omega - \omega_0))} \tag{5}$$

$$S_{22} = \frac{\nu_{22} + jT_c(\omega - \omega_c) - \frac{\alpha}{1+S}/(1 + jT_2(\omega - \omega_0))}{1 + jT_c(\omega - \omega_c) - \frac{\alpha}{1+S}/(1 + jT_2(\omega - \omega_0))} \tag{6}$$

$$S_{12} = \frac{\nu_{12}}{1 + jT_c(\omega - \omega_c) - \frac{\alpha}{1+S}/(1 + jT_2(\omega - \omega_0))}, \tag{7}$$

where the relation $\alpha/(1 + S) = R_a/(R_c(1 + \beta_1 + \beta_2))$ has been used. The ν_{ij} are simply functions of the coupling parameters. They are,

$$\nu_{11} = \frac{1 - \beta_1 + \beta_2}{1 + \beta_1 + \beta_2} \tag{8}$$

$$\nu_{22} = \frac{1 - \beta_2 + \beta_1}{1 + \beta_1 + \beta_2} \tag{9}$$

$$\nu_{21} = \nu_{12} = \frac{2\sqrt{\beta_1 \beta_2}}{1 + \beta_1 + \beta_2}. \tag{10}$$

The two critical frequencies of the system are the $(F = 1, m_F = 0) \rightarrow (F = 0, m_F = 0)$ hyperfine transition frequency, and the cavity resonant frequency,

ω_0 = the unpulled angular transition frequency of the atomic hydrogen

ω_c = the angular resonant frequency of the microwave cavity.

The relevant system time constants are,

T_1 = longitudinal time constant of the atomic hydrogen

T_2 = transverse time constant of the atomic hydrogen

T_c = the time constant of loaded cavity resonator i.e. $\hat{Z}_g, \hat{Z}_l = 1$

T_{cu} = the time constant of unloaded cavity resonator.

Other relevant system parameters are defined as follows:

$$\alpha = K Q_c T_1 T_2 I \qquad \text{oscillation threshold parameter}$$

$$\alpha = 1 \quad \text{at oscillation threshold, and } 0 \le \alpha < 1 \text{ for passive operation}$$

$$S = \frac{T_1 T_2 b^2}{1 + T_2^2 (\omega - \omega_0)^2} \qquad \text{the saturation factor}$$

$$Q_c = \frac{\omega_c T_c}{2} \qquad \text{loaded Q of the resonant cavity}$$

$$Q_a = \frac{\omega_0 T_2}{2} \qquad \text{Q of the atomic line}$$

$$K = \frac{\mu_0 \eta \mu_B^2}{\hbar V_c} \qquad \text{coupling parameter} \tag{11}$$

$\mu_0 = $ permeability of free space

$\mu_B = $ Bohr magneton

$V_c = $ the cavity volume

$\eta = $ the cavity filling factor

$\hbar = $ Planck's constant over 2π

$I = $ net atomic hydrogen flux in atoms/second

$b = $ amplitude of the cavity magnetic field.

Further details regarding these quantities are given in [1], [2], [4] and [5].

The scattering parameters are useful for precise calculation of the effects of microwave measurement errors on system performance. The principal errors of concern are those due to source and load mismatch, the effects of lossy transmission lines, residual reflections in the measurement path, limited measurement isolation or directivity, the effects of dispersion in the cavity resonator, and the effects of nearby cavity modes. All of these imperfections can be analyzed by properly modifying the two port scattering parameter model of the maser given in equations (4) through (7). Their effect on long term stability of the system can then be derived through sensitivity analyses.

In a system in which the generator and load reflection coefficients are Γ_g and Γ_l, respectively, we find that the measured value of S_{21} is given by

$$S_{21,m} = \frac{S_{21}}{1 - S_{11}\Gamma_g - S_{22}\Gamma_l + \Gamma_g \Gamma_l (S_{11}S_{22} - S_{21}S_{12})}, \tag{12}$$

where we have,

$$\Gamma_g = \frac{\hat{Z}_g - 1}{\hat{Z}_g + 1} \qquad and \qquad \Gamma_l = \frac{\hat{Z}_l - 1}{\hat{Z}_l + 1}. \tag{13}$$

Or, in terms of the normalized impedances, we obtain

125

$$S_{21,m} = \frac{\sqrt{\beta_1 \beta_2}}{2} \left(\frac{(\hat{Z}_g + 1)(\hat{Z}_l + 1)}{\hat{Z}_c + \hat{Z}_a + \beta_1 \hat{Z}_g + \beta_2 \hat{Z}_l} \right). \tag{14}$$

If $\hat{Z}_g$ and $\hat{Z}_l$ can be considered to have constant magnitude and phase over the frequency range of interest, then $S_{21,m}$ is seen to be inversely proportional to the total loop impedance seen from inside the cavity. Under these conditions, we can make the following approximation:

$$S_{21,m} \cong \frac{k}{\hat{Z}_T}, \tag{15}$$

where the total loop impedance, $\hat{Z}_T$ is given by,

$$\hat{Z}_T = \hat{Z}_c + \hat{Z}_a + \beta_1 \hat{Z}_g + \beta_2 \hat{Z}_l, \tag{16}$$

and k is a complex constant.

COMMON DETECTION TECHNIQUES

Two means of detection of the hyperfine resonance ω_0 are commonly considered, namely, maximum amplitude detection and phase inflection detection. The case of maximum amplitude detection is fairly intuitive. The discriminator characteristic becomes the first derivative of the magnitude of $S_{21,m}$ and we can set our crystal servo to lock to the point where this derivative is zero. This is equivalent to locating the frequency (ω_A) where,

$$\left. \frac{\partial |\hat{Z}_T|}{\partial \omega} \right|_{\omega_A} = 0. \tag{17}$$

For the condition of negligible saturation, this criterion produces a pulling factor of,

$$P_A = \frac{Q_c}{Q_a(2 - \alpha)}, \tag{18}$$

where the pulling factor P_A is defined as,

$$P_A \equiv \frac{\omega - \omega_0}{\omega_c - \omega_0}, \tag{19}$$

and ω_A is the detected frequency. The subscripts A and p differentiate between the different detection techniques.

If the detection criterion of phase inflection is used, we must force the servo to lock to the frequency (ω_p) at which,

$$\left. \frac{\partial^2 \varphi}{\partial \omega^2} \right|_{\omega_p} = 0,$$

where

$$\hat{Z}_T(\omega) \equiv \left| \hat{Z}_T(\omega) \right| e^{j\varphi(\omega)}. \tag{20}$$

This can be shown to yield a pulling factor P_p that is equal to the Q ratio,

$$P_p = \frac{Q_c}{Q_a}. \tag{21}$$

As the oscillation parameter α approaches unity in (18), P_A approaches P_p. In contrast, P_p is independent of α. Since the spin exchange contributions to the overall relaxation are small at low hydrogen flux we

126

can assume that Q_a remains constant as α is varied by changing the atomic flux. Thus, when the cavity is mistuned in a passive maser, the dependence of P_A on α would yield in the amplitude detection technique a sensitivity to flux variations not present with the phase detection technique.

Both the amplitude and the phase detection techniques can be implemented by applying a sinusoidally frequency modulated carrier to the hydrogen resonance, and detecting the amplitude modulation produced on the output signal. Ideally, there will be no amplitude modulation detected if the carrier frequency is equal to ω_0. The amplitude detection technique is implemented by modulating at frequencies less than the bandwidth of the hydrogen response whereas the phase technique is implemented by modulating at frequencies much greater than this bandwidth [6].

SWITCHED FREQUENCY MODULATION TECHNIQUES

We are presently using switched frequency modulation techniques to simulate various detection criteria. The experimental system is diagrammed in figure 2. The network analyzer is referenced to the slaved oscillator and is used to produce signals at fixed frequencies relative to the oscillator. Switched frequency modulation refers to the process of stepping a CW signal through a fixed set of discrete frequencies. The signal remains at a single frequency for a fixed interval of time during which some measurement is made. Usually the amplitude and/or phase of the steady state response is measured and then the next frequency is selected and the measurement is repeated. Using this technique, we build up a set of measurements of the steady state transfer function. These measurements contain information about the absolute frequency of the slaved oscillator relative to the hydrogen resonance line. By using frequencies well separated from the hydrogen line, so that only the cavity response is sensed, we obtain information about the cavity resonance relative to the crystal oscillator. All this information is used to control both the crystal and the cavity, closing both servo loops.

Using switched frequency techniques, we have tried three different schemes for detection of the hydrogen resonance. They are amplitude, phase and impedance detection. The amplitude and phase detectors are discrete simulations of the two detection schemes described in the previous section. They are implemented by sampling the transfer function and estimating either the first derivative of the amplitude or the second derivative of the phase of $S_{21,m}$. In both cases, the estimate of the derivative is used as the error signal in the servo. It can be shown that the pulling factor for these two techniques is essentially the same as their continuous modulation counterparts.

IMPEDANCE DETECTION

The impedance detection technique is implemented using switched frequency techniques. As its name implies, it is based on measurements of the total loop impedance $\hat{Z}_T$. The loop impedance is defined by (15) and (16). One can obtain this impedance by inverting the measurement of $S_{21,m}$ and setting the constant $k = 1$. In the present model, we will now assume that the external terminations are well matched. That is, $\hat{Z}_g$ and $\hat{Z}_l$ are real, frequency independent and equal to one. These effects can be lumped into the resistive part of the cavity impedance and the external terminations assumed to produce cavity loading but no cavity tuning. In view of these assumptions, one obtains

$$\hat{Z}_T = \hat{Z}_c + \hat{Z}_a + \beta_1 + \beta_2,$$
$$\hat{Z}_T \propto 1 + jT_c(\omega - \omega_c) - \frac{\alpha/(1 + S)}{1 + jT_2(\omega - \omega_0)}. \tag{22}$$

Figure 3 shows a plot of $\hat{Z}_T$ in the impedance plane for $S = 0$, and for the cavity mistuned by approximately half its bandwidth. Angular frequency is the parameter running upwards along the curve. Note that the phase and magnitude of the impedance at any frequency are easily obtained by drawing the vector from the origin to the point on the curve corresponding to that frequency. The measured magnitude and phase will be the magnitude and phase of that vector.

127

The curve is made up of two simple curves, a straight line running from $X = -\infty$ to $X = +\infty$, and a circle tangent to that line at $\omega = \omega_0$. The straight line is due to the cavity impedance, and the circle is due to the atomic impedance. The relative pulling factors of the different servos are easily seen from this diagram. The frequency at which the amplitude servo will lock is that point on the circle (ω_A) which makes the magnitude of the measurement vector a minimum. The phase servo will lock at the point on the circle (ω_p) at which the measured phase is equal to the phase of the point where the hydrogen circle and cavity baseline touch. The pulling factors of the different techniques are gauged by noting the relative distance along the hydrogen circle between the point of lock (either ω_A or ω_p) and ω_0. For the parameters represented by this particular impedance plot, it is apparent that the amplitude servo pulling factor is roughly half that of the phase servo.

This graphical interpretation of the pulling factor has led us to look for ways in which we could force the crystal servo to lock directly to ω_0. This would result in a pulling factor of zero simply because there would always be zero distance on the circle between the lock point and ω_0 regardless of the cavity mistuning. A similar technique for locking to ω_0 is described in [7].

With reference to the impedance plot of figure 4, the impedance detection technique is based upon the observation that a vector **A** tangent to the hydrogen circle will point parallel to the straight line of the cavity response only if the point of tangency is at ω_0. We formulate the servo condition then, such that **A** must be parallel to **B** if $\omega_x = \omega_0$. **B** is a vector which points in the direction of the straight line representing the cavity impedance. The servo system must be able to measure the vectors **A** and **B** and to adjust the crystal frequency ω_x so that **A** is held parallel to **B**.

To estimate the vectors **A** and **B**, the impedance $\hat{Z}_T$ is calculated at the following four frequencies:

$$\omega_1 = \omega_x - \delta$$
$$\omega_2 = \omega_x - \epsilon$$
$$\omega_3 = \omega_x + \epsilon$$
$$\omega_4 = \omega_x + \delta. \tag{23}$$

Here, ω_x is the crystal probe frequency and ϵ, δ are modulation frequencies producing test frequencies that are on and off the line, respectively. We now form **A** and **B** using $\hat{Z}_T(\omega)$ from (22). Let,

$$\mathbf{A} = \hat{Z}_T(\omega_3) - \hat{Z}_T(\omega_2)$$
$$\mathbf{B} = \hat{Z}_T(\omega_4) - \hat{Z}_T(\omega_1). \tag{24}$$

The condition that **A** be parallel to **B** is the same as $Im(AB^*) = 0$, where A and B are taken to be the complex form of the vectors. We calculate that,

$$Im(AB^*) = -\frac{8\alpha T_c T_2^2 \delta \epsilon (\omega_x - \omega_0)}{(1 + T_2^2(\omega_x - \omega_0 + \epsilon)^2)(1 + T_2^2(\omega_x - \omega_0 - \epsilon)^2)} \tag{25}$$

$$\cong -\frac{8\alpha T_c T_2^2 \delta \epsilon}{(1 + (T_2\epsilon)^2)^2}(\omega_x - \omega_0), \tag{26}$$

with the approximate form valid for $\omega_x - \omega_0 \ll \epsilon$. The expression $Im(AB^*)$ is zero for $\omega_x = \omega_0$, independent of the value of the cavity frequency. Therefore, we see that the impedance detection scheme should produce no cavity pulling.

EXPERIMENTAL VERIFICATION

We have empirically shown that there is a large reduction in cavity pulling when using the impedance detection scheme in the experimental setup shown in figure 2. The measurement of pulling factor was done by varying the cavity frequency by $\pm 2kHz$ about the cavity lock point and measuring the resulting change in output frequency when using a given detection scheme. In order to change detection schemes we simply hit a softkey on the controlling computer (no hardware attached to the maser need be changed). This eliminates the possibility that the cavity Q or tuning coefficients might change between measurements. We were able to measure a pulling factor of 2×10^{-14} per hertz of cavity tuning using amplitude detection and 5×10^{-16} per hertz of cavity tuning using impedance detection. This represents a reduction in pulling of a factor of 40.

The residual pulling that we see now is not completely explained. It could be related to saturation of the hydrogen line, delay in the measurement circuit, or dispersion in the sapphire cavity. Anything that would make the true transfer function differ from the ideal of figure 3 could cause some residual pulling and is therefore suspect. Efforts are now under way to eliminate the major sources of the residual pulling and thus reduce the cavity pulling by another factor of ten.

ACKNOWLEDGEMENTS

REFERENCES

[1] J.Viennet et al., "Cavity Pulling in Passive Frequency Standards," IEEE Trans. on Instrumentation and Measurement, Vol. IM–21, No. 3, Aug. 1972.

[2] P. Lesage and C. Audoin, "Amplitude Noise in Passively and Actively Operated Masers," Proc. of the 33rd Annual Symposium on Frequency Control, pp. 515–535, 1979.

[3] R. L. Kyhl et al., "Negative L and C in Solid State Masers." Proc. of the IRE, Vol. 50, No. 7, July 1962.

[4] D. Kleppner et al., "Theory of the Hydrogen Maser,"Phys. Rev., Vol. 126, No. 2, 603–615, April 15, 1962.

[5] D. Kleppner et al., "Hydrogen–Maser Principles and Techniques," Phys. Rev., Vol. 138, No. 4A, A972–A983, 17 May, 1965.

[6] G. Busca and H. Brandenberger, "Passive H Maser," Proc. of the 33rd Annual Symposium on Frequency Control, pp. 563–568, 1979.

[7] K. Uglow, "A Signal Processing Scheme for Reducing the Cavity Pulling Factor in Passive Hydrogen Masers," Proc. of the 18th Annual PTTI Applications and Planning Meeting, pp. 621–629, 1986.
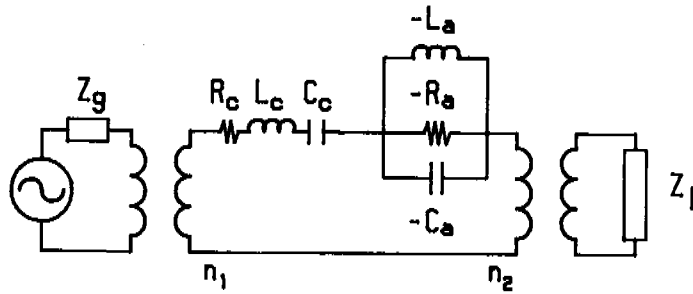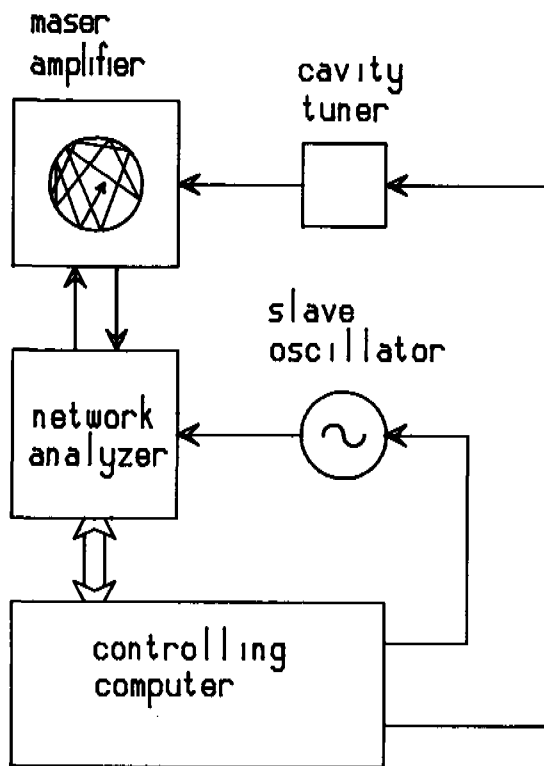
figure 1. Equivalent circuit of the passive maser

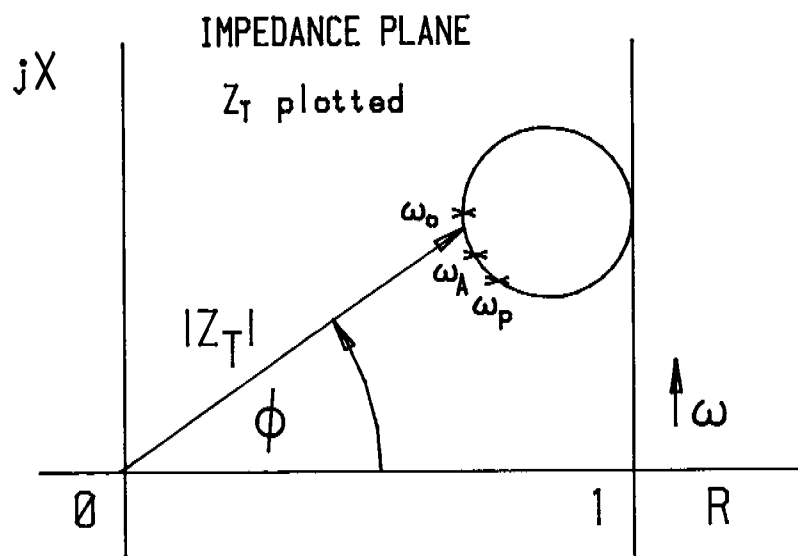figure 2. Block diagram of the experimental system

figure 3. Graph of Z_T in the impedance plane, showing the locations of ω_0, ω_A and ω_p.
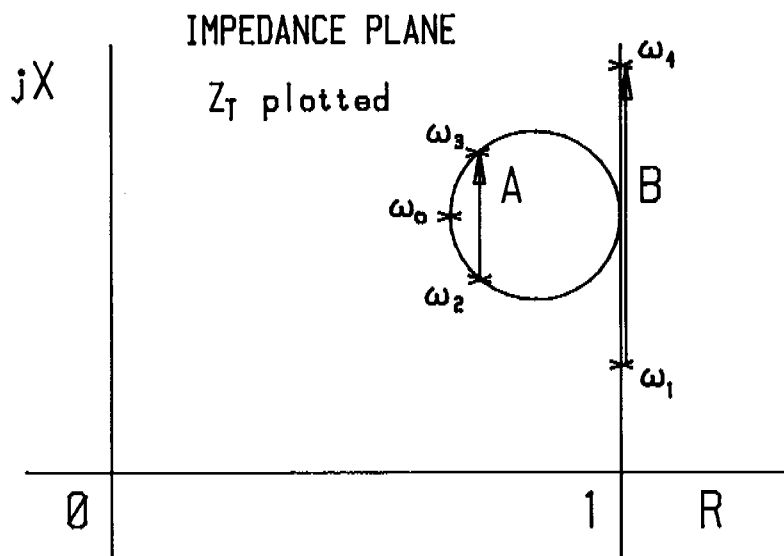

figure 4. Impedance plane diagram describing the impedance detection method.